

excess of KI, and titrating the liberated iodine with  $\text{Na}_2\text{S}_2\text{O}_3$  to a starch endpoint. Found: 15.15. The autoxidation product of a similar experiment gave a strong EPR signal at 77 K, with  $g_{\perp} = 2.08$ ,  $g_{\parallel} = 2.41$ . After the sample had been heated in vacuo for 2 h at 140 °C, the intensity of the EPR signal at 77 K was reduced by a factor of 12. Bulk susceptibility measurements on such heated residues in two experiments led to calculated magnetic moments of 0.19 and 0.31  $\mu_B$ , respectively. In one case, the sample lost 3.7 wt % water, which was condensed in a cold trap ( $\eta_D^{29}$  1.331, lit. 1.332). The absorption at 3400  $\text{cm}^{-1}$  disappeared when the water had been volatilized but new peaks appeared at 1520 and 610  $\text{cm}^{-1}$ . In another case, the copper(II) content after heating was found to be 4.5%.

**Autoxidation of 0.60Cu/0.40CuCl/MeEtImCl.** In the same way, in a typical experiment, 7.241 g (4.3 mL) of fused salt of composition 0.600 mole fraction of CuCl, containing 36.81 mmol of copper(I), took up 4.60 mmol of  $\text{O}_2$ . The final nominal composition was 1/0.667/0.125 CuCl/MeEtImCl/ $\text{O}_2$ ,  $M_r$  200.7,  $\chi_g = +1.178 \times 10^{-6}$ , diamagnetic correction  $-0.545 \times 10^{-6}$ ,  $\chi_g^{\text{cor}} = +1.723 \times 10^{-6}$ ,  $\chi_M^{\text{cor}} = 345.9 \times 10^{-6}$  cgsemu,  $\mu_{\text{eff}}$  0.90  $\mu_B$ . The IR spectrum of the black liquid was virtually identical with that of the starting material, with only a slight absorption at 3400  $\text{cm}^{-1}$  and an extremely weak absorption at 1660  $\text{cm}^{-1}$ .

**1-Methyl-3-ethylimidazolone.** The autoxidation product of a 0.40/0.60 CuCl/MeEtImCl melt was placed in a continuous extractor with water and extracted with ether. The extract was evaporated and the residue dried with 4A molecular sieve:  $^1\text{H NMR}$  ( $\text{CD}_3\text{CN}$ )  $\delta$  1.10 (3 H, t,  $J = 6$  Hz,  $\text{CH}_2\text{CH}_3$ ), 3.05 (3 H, s,  $\text{CH}_3$ ), 3.47 (2 H, q,  $J = 6$  Hz,  $\text{CH}_2\text{CH}_3$ ), 6.20 (2 H, m,  $\text{CH}=\text{CH}$ ); MS,  $m/e$  (rel intensity) 127 (10), 126 (90),  $M^+$ , calcd. 126), 125 (8), 111 (21), 98 (35), 97 (11), 83 (4.5), 74 (40), 69 (17), 62 (10), 61 (100), 60 (20), 56 (13), 55 (4.1), 45 (17), 44 (49), 43 (85), 42 (36), 41 (8.4); IR (thin film) 3160 (w), 3118 (s,  $\text{H}-\text{C}=\text{C}$ ), 3095 (sh), 2925 (s), 2450 (w), 1660 (vs, br,  $\text{C}=\text{O}$ ), 1460 (vs, br), 1405

(vs), 1375 (m), 1295 (w), 1240 (s,  $\text{N}-\text{CH}_3$ ), 1218 (s,  $\text{N}-\text{C}_2\text{H}_5$ ), 1098 (m), 1042 (m), 1012 (m), 945 (m), 810 (s), 780 (w), 747 (s), 665 (s, br), 600  $\text{cm}^{-1}$  (m).

**Reaction with 2,6-Dimethylphenol.** Approximately 4 g each of various fused salt autoxidation products and of 2,6-dimethylphenol were stirred under nitrogen at various temperatures in the range 32–45 °C for 1 h. The reaction mixture was added to 50 mL of methanol plus 1 mL of concentrated HCl, the solution was cooled in an ice/salt bath, 75 mL of water was added in portions, and the mixture was filtered. The precipitate from reactions using  $n = 0.40$  autoxidation products was poly(2,6-dimethylphenylene oxide). Its discoloration due to copper salts could be removed by washing with dilute HCl, to give a yellow-white polymer that darkened on standing in air. Reactions using the  $n = 0.60$  autoxidation products at the higher temperatures gave the red crystalline 2,2',6,6'-tetramethyldiphenquinone, mp 208 °C (lit.<sup>15-17</sup> 214 °C), while mixtures of polymer and the quinone were obtained under intermediate conditions.

**Oxidation of 1-Methyl-3-ethylimidazolium Chloride.** When a mixture of 1.38 g (10.2 mmol) of anhydrous copper(II) chloride, 2.45 g (30.8 mmol) of copper(II) oxide, and 3.00 g (20.5 mmol) of MeEtImCl was heated to 110 °C in vacuo, a black liquid was formed. The water evolved over 2 h was condensed in a cold trap; it weighed 0.155 g (8.60 mmol) yield, 84% based on eq 4. The infrared spectrum of the residue showed the characteristic absorptions of 1-methyl-3-ethylimidazolone.

**Acknowledgment.** We thank Scott Goodman and Gregory Witkop for experimental assistance in the work with 2,6-dimethylphenol.

**Registry No.** CuCl, 7758-89-6; MeEtImCl, 65039-09-0;  $\text{O}_2$ , 7782-44-7;  $\text{H}_2\text{O}$ , 7732-18-5; 1-methyl-3-ethylimidazolone, 103816-76-8; 2,6-dimethylphenol, 576-26-1; polyphenylene oxide, 9041-80-9; quinone, 106-51-4.

Contribution from the Laboratoire de Cristallographie aux Rayons X, Université de Genève, CH-1211 Genève 4, Switzerland, and Materials Science and Technology Division and Intense Pulsed Neutron Source Program, Argonne National Laboratory, Argonne, Illinois 60439

## Structural Studies of the Hydrogen Storage Material $\text{Mg}_2\text{NiH}_4$ . 2. Monoclinic Low-Temperature Structure

P. Zolliker,<sup>†</sup> K. Yvon,<sup>\*†</sup> J. D. Jorgensen,<sup>‡</sup> and F. J. Rotella<sup>§</sup>

Received March 28, 1986

The structure of the low-temperature phase of  $\text{Mg}_2\text{NiD}_4$  was determined from time-of-flight neutron powder diffraction data collected at 298 K. It has monoclinic symmetry (space group  $C2/c$ ,  $a = 14.343$  (5) Å,  $b = 6.4038$  (10) Å,  $c = 6.4830$  (13) Å,  $\beta = 113.52$  (4)°,  $Z = 8$ ) and contains four symmetry-independent D atoms. As expected, the D atoms surround the Ni atoms in a nearly regular tetrahedral configuration (average bond lengths Ni–D = 1.54 Å, average bond angles D–Ni–D = 109.4°). Microtwinning parallel to (011) leads to severe anisotropic broadening of the diffraction peaks.

### Introduction

$\text{Mg}_2\text{NiH}_4$  has been considered as a promising material for hydrogen storage applications, such as in fuel tanks for hydrogen-powered vehicles.<sup>1</sup> Its structure transforms between 240 and 210 °C from a cubic high-temperature ( $\beta'$ ) modification into a monoclinic low-temperature ( $\beta$ ) modification.<sup>2</sup> As shown in the first paper of this series,<sup>3</sup> and later by other workers,<sup>4-6</sup> the high-temperature structure consists of a  $\text{CaF}_2$  type metal atom arrangement in which the D atoms surround the Ni atoms in a disordered configuration. As to the room-temperature structure, conflicting results were reported in the literature (for a review see ref 7). The metal atom substructure as determined from X-ray powder diffraction analysis was described in terms of various models and space groups ( $C2/m$ ,<sup>8</sup>  $Ja$ ,<sup>9</sup>  $Cc$ <sup>10</sup>). Diffraction maxima that could not be interpreted by these models were ascribed to a second low-temperature modification of orthorhombic symmetry.<sup>10</sup> The distribution of the hydrogen atoms was determined

by two independent neutron diffraction experiments on the deuteride and found to be ordered in one study<sup>11</sup> and disordered in another.<sup>12</sup> In the former study a model consisting of a square-planar deuterium atom configuration around the Ni atoms was

- (1) Buchner, H. In *Proceedings of the 2nd World Hydrogen Energy Conference, Zürich, Switzerland, 1978*; Veziroglu, N., Seifritz, W., Eds.; Pergamon: Elmsford, NY, and Oxford, England, 1978; Vol. 4, p 1749.
- (2) Gavva, Z.; Mintz, M. H.; Kimmel, G.; Hadari, Z. *Inorg. Chem.* **1979**, *18*, 3595.
- (3) Yvon, K.; Schefer, J.; Stucki, F. *Inorg. Chem.* **1981**, *20*, 2776. For preliminary results see also: Schefer, J.; Fischer, P.; Hälg, W.; Stucki, F.; Schlapbach, L.; Didisheim, J.-J.; Yvon, K.; Andresen, A. F. *J. Less-Common Met.* **1980**, *74*, 65.
- (4) Noréus, D.; Olssen, L. G. *J. Chem. Phys.* **1983**, *78*, 2419.
- (5) Soubeyroux, J. L.; Fruchart, D.; Mikou, A.; Pezat, M.; Darriet, B.; Hagenmuller, P. *Mater. Res. Bull.* **1984**, *19*, 969.
- (6) Zolliker, P.; Yvon, K. *Mater. Res. Bull.* **1986**, *21*, 415.
- (7) Yvon, K. *J. Less-Common Met.* **1984**, *103*, 53.
- (8) Noréus, D.; Werner, P.-E. *Mater. Res. Bull.* **1981**, *16*, 199.
- (9) Ono, S.; Hayakawa, H.; Suzuki, A.; Nomura, K.; Nishimiya, N.; Tabata, T. *J. Less-Common Met.* **1982**, *88*, 63.
- (10) Hayakawa, H.; Ishido, Y.; Nomura, K.; Uruno, H.; Ono, S. *J. Less-Common Met.* **1984**, *103*, 277.
- (11) Noréus, D.; Werner, P.-E. *J. Less-Common Met.* **1984**, *97*, 215.
- (12) Soubeyroux, J. L.; Fruchart, D.; Mikou, A.; Pezat, M.; Darriet, B. *Mater. Res. Bull.* **1984**, *19*, 1119.

<sup>†</sup> Université de Genève.

<sup>‡</sup> Materials Science and Technology Division, Argonne National Laboratory.

<sup>§</sup> Intense Pulsed Neutron Source Program, Argonne National Laboratory.

refined on a subcell only against data of medium resolution ( $a = 6.496 \text{ \AA}$ ,  $b = 6.412 \text{ \AA}$ ,  $c = 6.602 \text{ \AA}$ ,  $\beta = 93.23^\circ$ , space group  $C2/m$ ,  $Z = 4$ ,  $(\sin \theta)/\lambda_{\text{max}} = 0.54 \text{ \AA}^{-1}$ , and  $R_F = 0.12$  for 10 atomic positional parameters<sup>11</sup>, while in the latter study a model consisting of a disordered octahedral configuration was refined against data of low resolution ( $a = 13.201 \text{ \AA}$ ,  $b = 6.407 \text{ \AA}$ ,  $c = 6.491 \text{ \AA}$ ,  $\beta = 93.21^\circ$ , space group  $Cc$ ,  $Z = 8$ ,  $(\sin \theta)/\lambda_{\text{max}} = 0.32 \text{ \AA}^{-1}$ , and  $R = 0.10$  for 51 atomic positional parameters<sup>12</sup>). Both models were unlikely, the former because of the absence of square-planar coordinated systems based on  $d^{10}$  ions and the latter because of its deuterium atom disorder. Recently the metal atom arrangement of  $\beta\text{-Mg}_2\text{NiD}_4$  was reinvestigated by X-ray powder diffraction profile analysis at room temperature.<sup>13</sup> In contrast to the previous studies, a centrosymmetric structural model was refined that took into account both anisotropic line broadening and additional diffraction peaks due to microtwinning ( $a = 14.36 \text{ \AA}$ ,  $b = 6.41 \text{ \AA}$ ,  $c = 6.49 \text{ \AA}$ ,  $\beta = 113.6^\circ$ , space group  $C2/c$ ,  $Z = 8$ ,  $(\sin \theta)/\lambda_{\text{max}} = 0.50 \text{ \AA}^{-1}$ ,  $R_p = 0.12$ , and  $R_F = 0.04$  for 8 atomic positional parameters<sup>13</sup>). While the overall metal atom configuration obtained was similar to those of the noncentrosymmetric models, the accuracy of atomic positions was higher by a factor of 2 and 5, on the average, with respect to those in ref 10 and 9, respectively. The centrosymmetric structure (space group  $C2/m$ ) reported in ref 8 was considered unsatisfactory because it did not explain a series of weak diffraction lines. In view of these results a reinvestigation of the deuterium atom distribution in  $\text{Mg}_2\text{NiD}_4$  was desirable. In this paper we report the results of a structure refinement based on high-resolution time-of-flight (TOF) neutron powder diffraction data.

### Experimental Section

The sample used for the neutron diffraction study was identical with that used in the X-ray diffraction study (sample no. 2 in ref 13). It contained  $\text{MgD}_2$  as impurity phase, and the  $\text{Mg}_2\text{NiD}_4$  phase was characterized by the presence of microtwinning, which leads to anisotropic broadening of the diffraction peaks. Approximately 3 g of the sample was packed into a thin-walled, 11 mm diameter, 50 mm long vanadium can that was sealed under an argon atmosphere. Data were collected at room temperature on the Special Environment Powder Diffractometer (SEPD)<sup>14</sup> at Argonne's Intense Pulsed Neutron Source (IPNS) for about 35 h. The SEPD is a time-of-flight powder diffractometer with multi-detector arrays at fixed scattering angles ( $2\theta$ ) of 150, 90, 60, 30, and  $14^\circ$ . For structural refinement, the high-resolution data from the back-scattering,  $150^\circ$ , detector banks were used. Neutron scattering lengths<sup>15</sup> used ( $10^{-12} \text{ cm}$ ): 1.03 for Ni; 0.538 for Mg; 0.667 for D. The various TOF neutron powder diffraction intensity profiles are represented in Figure 1. They are grouped into three TOF ranges, each having its own intensity scale and covering different interplanar spacings. The spectra show (a) the raw intensity data, (b) the background contribution, (c) the contribution of the refined  $\text{Mg}_2\text{NiD}_4$  phase, (d) the contribution of the  $\text{MgD}_2$  impurity phase, and (e) the difference between calculated and observed intensity profiles (for (b)–(e) see Results).

### Results

Initial attempts at analysis were performed by using the Rietveld method<sup>16</sup> for time-of-flight data<sup>17</sup> for multiple-phase samples<sup>18</sup> as used at the IPNS facility.<sup>19</sup> Various structure models were tested on the basis of the metal atom positions previously determined from the X-ray study.<sup>13</sup> However, none of the refinements converged, presumably because of the neglect of anisotropic peak

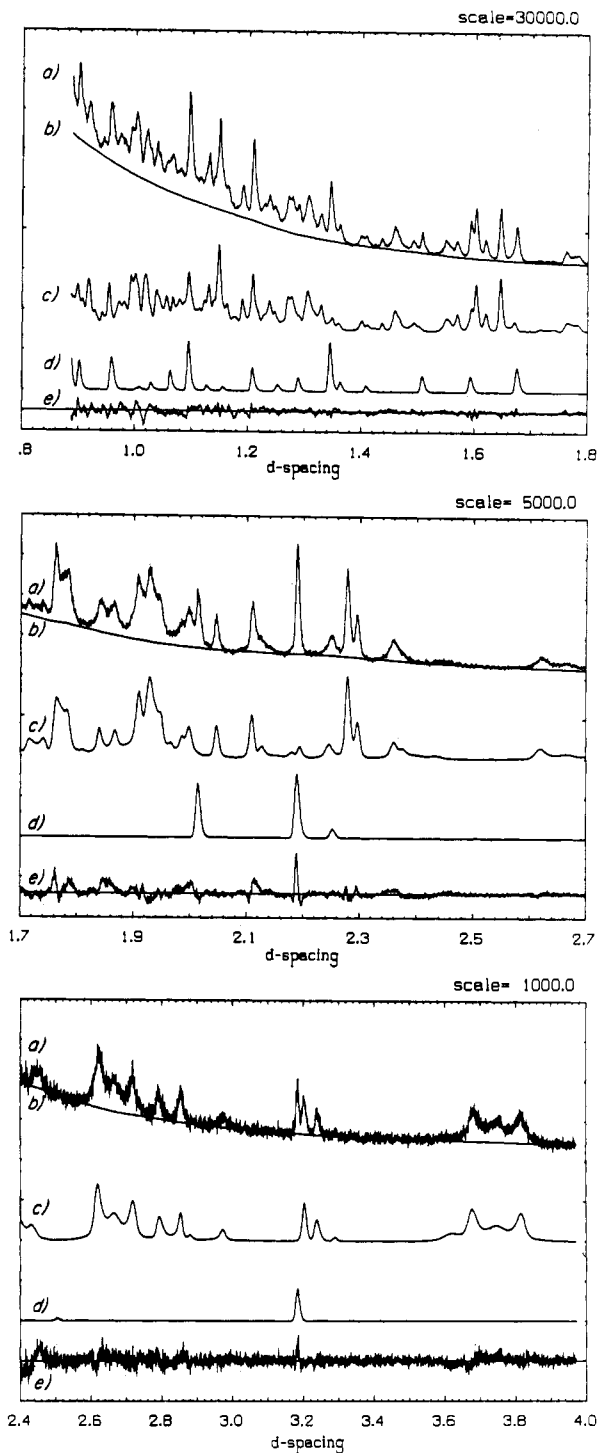


Figure 1. Neutron time-of-flight powder diffraction patterns at  $2\theta = 150^\circ$  for  $\text{Mg}_2\text{NiD}_4$ . For description, see text.

broadening due to microtwinning, which could not be handled by the TOF Rietveld computer code available.<sup>19</sup> Subsequently, the contribution of the  $\text{MgD}_2$  phase, which was fit reasonably well in the above two-phase Rietveld analysis, was subtracted from the  $150^\circ$  raw TOF data, and the resulting single-phase  $\text{Mg}_2\text{NiD}_4$  data were transformed to a powder diffraction pattern at fixed neutron wavelength ( $0.5 \text{ \AA}$ ). The transformed data were corrected for background and analyzed by the same profile refinement technique<sup>20</sup> as that used for analysis of the X-ray diffraction data.<sup>13</sup> This technique allowed for anisotropic line broadening as described previously.<sup>13</sup> Again, several structural models were tested in space

- (13) Zolliker, P.; Yvon, K.; Baerlocher, C. *J. Less-Common Met.* **1986**, *115*, 68.  
 (14) Jorgensen, J. D.; Faber, J., Jr. In "Proceedings of the Sixth Meeting of the International Collaboration on Advanced Neutron Sources"; Report ANL-82-80; Argonne National Laboratory: Argonne, IL, 1983; p 105.  
 (15) Koester, L.; Steyerl, A. *Neutron Physics*; Modern Tracts of Physics, Vol. 80; Springer: Berlin and Heidelberg, 1977.  
 (16) Rietveld, H. M. *J. Appl. Crystallogr.* **1969**, *2*, 65.  
 (17) von Dreele, R. B.; Jorgensen, J. D.; Windsor, C. G. *J. Appl. Crystallogr.* **1982**, *15*, 157.  
 (18) Rotella, F. J. *Program and Abstracts*, American Crystallographic Association Annual Meeting, Stanford University, Stanford, CA, 1985; American Institute of Physics: New York, 1985; Series 2, Vol. 13, p 70.  
 (19) Rotella, F. J. *User Manual for Rietveld Analysis of Time-of-Flight Neutron Powder Diffraction Data at IPNS*; Argonne National Laboratory: Argonne, IL, 1983.

- (20) Baerlocher, C. *X-ray Rietveld System XRS-82*; Institut für Kristallographie: ETH-Zentrum, Zürich, 1982.

**Table I.** Structure Data for LT-Mg<sub>2</sub>NiD<sub>4</sub><sup>a</sup>

space group: *C2/c* (No. 15)  
 cell params:  $a = 14.343$  (5) Å,  $b = 6.4038$  (10) Å,  $c = 6.4830$  (13) Å,  $\beta = 113.52$  (4)°;  $(a/2)(\sin \beta) = 6.5755$  (10)

Positional and Isotropic Thermal Parameters				
	<i>x</i>	<i>y</i>	<i>z</i>	$\langle u^2 \rangle$ , Å <sup>2</sup>
Ni in (8f)	0.1194 (6)	0.2308 (11)	0.0832 (12)	-0.004 (2)
Mg(1) in (8f)	0.2652 (10)	0.4827 (24)	0.0754 (22)	-0.002 (2)
Mg(2) in (4e)	0	0.0144 (33)	0.25	-0.002 <sup>b</sup>
Mg(3) in (4e)	0	0.5130 (31)	0.25	-0.002 <sup>b</sup>
D(1) in (8f)	0.2113 (14)	0.2995 (26)	0.3037 (28)	0.032 (4)
D(2) in (8f)	0.1360 (12)	0.3163 (18)	0.8811 (23)	0.013 (2)
D(3) in (8f)	0.0105 (11)	0.2868 (19)	0.0537 (22)	0.013 <sup>b</sup>
D(4) in (8f)	0.1306 (12)	0.9950 (19)	0.0815 (23)	0.013 <sup>b</sup>

<sup>a</sup> Figures in parentheses are esd's: Those for the atomic parameters are calculated by the Rietveld program<sup>16,20</sup> and multiplied by a factor 2.5 as proposed by Scott;<sup>21</sup> those of the cell parameters are estimated from the accuracy of the twinning model. <sup>b</sup> Constrained.

group *C2/c* by assuming various distributions of deuterium atoms, including ordered tetrahedral and square-planar configurations and disordered deuterium distributions around the Ni atoms. Only the model with tetrahedral deuterium atom configuration refined successfully, leading to the agreement factors  $R_F = 4.4\%$  and  $R_{wp} = 13.8\%$  ( $R_{exp} = 5.7\%$ ) for 31 refined parameters (24 atomic parameters, 4 cell parameters, and 3 profile parameters). A total of 394 Mg<sub>2</sub>NiD<sub>4</sub> reflections with  $d$  values in the range of 0.89–2.5 Å were used in the profile refinement. Some of the individual temperature factors were constrained ( $\langle u^2 \rangle_{Mg(2)} = \langle u^2 \rangle_{Mg(1)}$  and  $\langle u^2 \rangle_{D(4)} = \langle u^2 \rangle_{D(3)} = \langle u^2 \rangle_{D(2)}$ ). The structure parameters obtained are summarized in Table I. An additional refinement of the deuterium occupancy factors showed no significant deviation from unity, and a refinement in the noncentrosymmetric space group *Cc* did not change the atom configuration significantly, nor did it improve the fit. In view of systematic errors due to absorption and extinction effects (see below), the anomalously low temperature factors of the metal atoms and the high temperature factor of one of the deuterium atoms (D(1)) may not be significant.

For  $d$  values above about 2.5 Å, the observed intensities were found to be systematically lower than those calculated with the structure model refined above, due to systematic effects such as absorption and extinction, leading to a poor  $R_{wp}$  factor of 30% for the entire  $d$  value range (0.89–3.97 Å). A comparison with low-resolution angle dispersive (AD) neutron diffraction data (P. Fischer, J. Schefer, unpublished results, 1979) suggested that these effects were specific for the TOF measurement (i.e., they depend on wavelength). The dependence of the structure factor ratio  $F^2_{TOF}/F^2_{AD}$  of corresponding diffraction peaks allowed for the determination of a correction function that explained well the observed lowering of the experimental intensities for high  $d$  values ( $I_{cor} = I_{calcd}/(1 + 1.04(d - 1.965 \text{ Å})^2)$  for  $d > 1.965$  Å). With this correction and an additional overall temperature factor (0.003 Å<sup>2</sup>), the structure model presented in Table I gave a good fit for the entire  $d$  range of the TOF data, as can be seen in Figure 1 and from the profile  $R$  factor ( $R_{wp} = 14.4\%$ ,  $R_{exp} = 7.0\%$ ) for  $0.89 < d < 3.97$  Å).

While the metal atom coordinates (see Table I) do not differ significantly from those obtained from the X-ray powder profile refinement,<sup>13</sup> the deuterium atom positions differ significantly from those reported in the two previous neutron diffraction studies.<sup>11,12</sup> As shown in Figure 2 the D atoms are ordered such that they surround the Ni atoms in nearly regular tetrahedral configurations. As shown in more detail in Figure 3a, each D atom is bonded to one Ni atom and has either four (D(2), D(3), D(4)) or three (D(1)) nearest Mg atom neighbors. The Ni–D bond lengths are 1.572 (20), 1.524 (16), 1.538 (16), and 1.519 (14) Å (for esd's see footnote a in Table I) for D(1), D(2), D(3), and D(4), respectively,

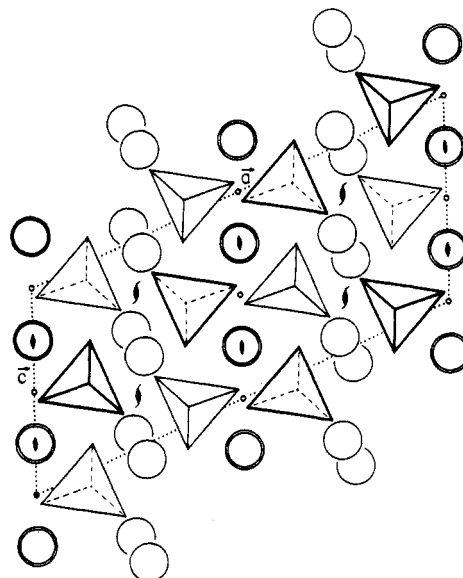


**Figure 2.** Monoclinic low-temperature structure of Mg<sub>2</sub>NiD<sub>4</sub> at  $T = 298$  K, viewed along the twofold axis ( $b$ ). Ni<sub>4</sub> units are shown as filled tetrahedra (light contours, centers at  $y \approx 1/4$ ; heavy contours, centers at  $y \approx 3/4$ ), and Mg as large circles (at  $y \approx 0$  or  $y \approx 1/2$ ). A double circle denotes two Mg (at  $y \approx 0$  and  $y \approx 1/2$ ). For symmetry elements other than inversion centers at  $y = 0$  and  $1/2$  (small circles), twofold axes, and screw axes see ref 22.

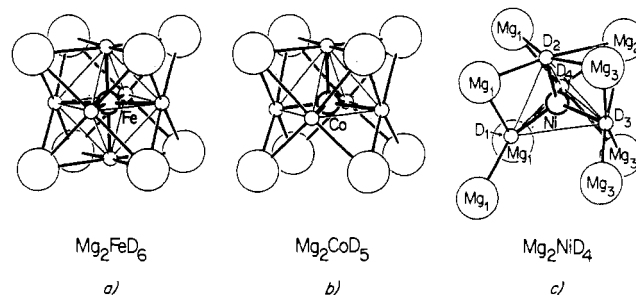


**Figure 3.** Structure units of (a) Mg<sub>2</sub>FeD<sub>6</sub>, (b) Mg<sub>2</sub>CoD<sub>5</sub>, and (c) Mg<sub>2</sub>NiD<sub>4</sub>.

while the D–Ni–D bond angles range from 107 to 110°, except for D(1)–Ni–D(3) (119.3 (10)°) and D(1)–Ni–D(4) (103.3 (10)°). The shortest Mg–D distance (Mg(3)–D(3) = 1.97 (2) Å) is similar to that in the elemental hydride MgD<sub>2</sub> (Mg–D = 1.95 (2) Å),<sup>23</sup> while the shortest separation between the D atoms (D–D = 2.43 (2) Å) is consistent with those found in other ternary metal hydride structures.<sup>7</sup>

### Discussion

The results of the above analysis confirm that the phase transformation in Mg<sub>2</sub>NiH<sub>4</sub> is essentially due to an order–disorder transition of the hydrogen atoms. During this transition the cubic CaF<sub>2</sub> type metal atom substructure of the high-temperature modification (every second Mg atom cube centered by a nickel atom) undergoes a monoclinic distortion, which is presumably due to steric hindrance resulting from the accommodation of tetrahedral H atom configurations in the Mg atom cubes. As shown in Figure 3c, three of the D atoms (D(2), D(3), D(4)) are located near the face centers of the (deformed) cube, such that these atoms form nearly tetrahedral angles with the Ni atom, whereas the fourth D atom (D(1)) is located away from a face center, thereby strongly displacing one of the metal atoms (Mg(1)). A comparison with the recently discovered ternary metal hydrides Mg<sub>2</sub>CoH<sub>5</sub><sup>25</sup>

(21) Scott, H. G. *J. Appl. Crystallogr.* **1983**, *16*, 159.

(22) International Union of Crystallography. *International Tables for Crystallography*; Reidel: Dordrecht, 1983; Vol. A.

(23) Zachariasen, W. H.; Holley, C. E., Jr.; Stamper, J. F., Jr. *Acta Crystallogr.* **1963**, *16*, 352.

(24) Didisheim, J.-J.; Zolliker, P.; Yvon, K.; Fischer, P.; Schefer, J.; Gubelmann, M.; Williams, A. F. *Inorg. Chem.* **1984**, *23*, 1953.

(25) Zolliker, P.; Yvon, K.; Fischer, P.; Schefer, J. *Inorg. Chem.* **1985**, *24*, 4177.

(Figure 3b) and  $\text{Mg}_2\text{FeH}_6^{24}$  (Figure 3a) shows that the deuterium atom configuration around the transition metal changes from tetrahedral (Ni ( $d^{10}$ )) to square-pyramidal (Co ( $d^8$ )) and octahedral (Fe ( $d^6$ )), in agreement with predictions from the 18-electron rule<sup>26</sup> and configurations found in other related ternary hydrides.<sup>27</sup> Thus the previously reported square-planar<sup>11</sup> or disordered<sup>12</sup> deuterium atom configurations around the Ni atoms in  $\beta\text{-Mg}_2\text{NiH}_4$  can probably be ruled out. The latter studies presumably suffered from the low resolution of the diffraction data and the deficiencies of the structural models, which underlines the importance of using powder diffraction data of high resolution for the refinement of complex structures.

Magnetic measurements on a sample of composition  $\text{Mg}_2\text{NiH}_{3.8}$  suggested that the susceptibility of the  $\text{Mg}_2\text{NiH}_4$  phase was nearly zero.<sup>28</sup> This result is consistent with the above structure containing  $d^{10}$  nickel atoms in tetrahedral configuration, for which diamagnetism is expected. Furthermore the dark red color of fully hydrided samples as well as X-ray photoelectron spectroscopy analysis and theoretical band structure calculations<sup>29</sup> suggested that  $\text{Mg}_2\text{NiH}_4$  is nonmetallic. These results are in agreement with a limiting ionic bond description based on  $\text{Mg}^{2+}$  cations and  $[\text{NiH}_4]^{4-}$  anions (the actual charges are of course different). However, since the above band structure calculations were performed on the (cubic)  $\beta'$  modification by assuming octahedral deuterium configurations, they may not apply to the (monoclinic)  $\beta$  modification on which the X-ray emission spectroscopy measurements were performed.<sup>29</sup> As to the NMR results published in ref 30,31, they probably need to be reinterpreted in view of the

structure model proposed above.

Finally, an analysis of the maximum hydrogen content of  $\text{Mg}_2\text{NiH}_4$  in terms of the so-called geometrical model<sup>32</sup> shows that its structure could accommodate two more H atoms per formula unit than found experimentally, similar to the structure of  $\text{Mg}_2\text{CoH}_5$ ,<sup>25</sup> which could accommodate one more H atom per formula unit. This demonstrates that the hydrogen content in these compounds is controlled by electronic rather than geometrical factors.

In conclusion we note that the knowledge of the hydrogen atom distribution in  $\text{Mg}_2\text{NiH}_4$  is essential for theoretical energy band calculations, which in turn may give better insight into the chemistry and properties of this technologically important hydrogen storage material.

**Acknowledgment.** We wish to acknowledge the support of the U.S. Department of Energy, BES-Materials Science (Contract No. W-31-109-ENG-38) for the neutron diffraction measurements at the Intense Pulsed Neutron Source, which is operated as a user facility. P.Z. wishes to thank Ch. Baerlocher and the Institut für Kristallographie und Petrographie for help and hospitality during the structure refinements made at ETH Zürich. This work has been supported by the Swiss National Energy Research Foundation and the Swiss National Science Foundation.

**Registry No.**  $\text{Mg}_2\text{Ni}$ , 12057-65-7;  $\text{Mg}_2\text{NiD}_4$ , 77340-45-5.

**Supplementary Material Available:** Tables of raw neutron diffraction data and the results of the structure refinement, including structural data, interatomic distances, selected bond angles, R factors, and background values (11 pages); a table of structure factors (4 pages). Ordering information is given on any current masthead page.

(26) Mingos, D. M. P. *Struct. Bonding (Berlin)* 1986, 63.

(27) Bau, R.; Chiang, M.Y.; Ho, D. M.; Gibbins, S. G.; Emge, T. J.; Koetzle, T. F. *Inorg. Chem.* 1984, 23, 2823.

(28) Stucki, F.; Schlapbach, L. *J. Less-Common Met.* 1980, 74, 143.

(29) Gupta, M.; Belin, E.; Schlapbach, L. *J. Less-Common Met.* 1984, 103, 389.

(30) Genossar, J.; Rudman, P. S. *J. Phys. Chem. Solids* 1981, 42, 611.

(31) Senegas, J.; Pezat, M.; Darnaudery, J. P.; Darriet, B. *J. Phys. Chem. Solids* 1981, 42, 29.

(32) Westlake, D. G. *J. Less-Common Met.* 1980, 75, 177.

Contribution from the Department of Chemistry,  
University of the West Indies, Kingston, Jamaica, West Indies

## Dinuclear Complexes of Transition Metals Containing Carbonate Ligands. 6.<sup>1</sup> Synthesis, Characterization, and Thermodynamic Studies of Dinuclear Complexes of Cobalt(III) Containing Bridging Hydroxide and Carbonate in Acidic Aqueous Solution

Garfield Sadler and Tara P. Dasgupta\*

Received February 12, 1986

Three new dinuclear cobalt(III) complexes containing carbonate as bridging group were prepared. The complexes are of the type  $[(\text{N})_3\text{Co}(\mu\text{-CO}_3)(\mu\text{-OH})(\mu\text{-X})\text{Co}(\text{N})_3]^{2+}$  where  $(\text{N})_3$  stands for either dien (1,5-diamino-3-azapentane) or  $(\text{NH}_3)_3$  and X is OH,  $\text{NH}_2$ , or  $\text{NO}_2$ . The complexes were characterized by UV-visible and infrared spectroscopy. These complexes equilibrate rapidly in acidic aqueous solution with  $[(\text{N})_3(\text{H}_2\text{O})\text{Co}(\mu\text{-CO}_3)(\mu\text{-X})\text{Co}(\text{N})_3(\text{OH}_2)]^{3+}$ . The thermodynamic parameters  $K$ ,  $\Delta H^\circ$ , and  $\Delta S^\circ$  were determined for these equilibrium reactions, and the results are compared with the thermodynamic parameters for some related dinuclear complexes.

### Introduction

During the last 5 years we have been interested<sup>2-4</sup> in preparing some novel dinuclear complexes of cobalt(III) containing carbonate as a bridging ligand. In 1981 we made first report of the carbonate-bridged dinuclear cobalt(III) complex  $[(\text{NH}_3)_3\text{Co}(\mu\text{-CO}_3)(\mu\text{-OH})_2\text{Co}(\text{NH}_3)_3]^{3+}$ . The compound was characterized<sup>2</sup>

by a three-dimensional X-ray diffraction study. Recently we were able to modify our synthetic approach due to our greater understanding of the characteristics of tribridged cobalt(III) complexes and, hence, were able to synthesize a series of novel dinuclear complexes with carbonate as bridging ligand. We report here the synthesis and characterization of these complexes and their thermodynamic properties in aqueous solution.

### Experimental Section

**Preparation of Complexes.** Preparation of Tris( $\mu$ -hydroxo)bis(tri-aminocobalt(III)) Perchlorate Dihydrate ("Triol"),  $[(\text{NH}_3)_3\text{Co}(\mu\text{-OH})_3\text{Co}(\text{NH}_3)_3](\text{ClO}_4)_2 \cdot 2\text{H}_2\text{O}$ . The compound was prepared by following the method of Linhard and Siebert.<sup>5</sup> The purity of the compound was

(1) Part 5: Koshy, K.; Dasgupta, T. P. *Inorg. Chim. Acta* 1986, 117, 111.

(2) Churchill, M. R.; Lashewycz, R.; Koshy, K.; Dasgupta, T. P. *Inorg. Chem.* 1981, 20, 376.

(3) Koshy, K.; Dasgupta, T. P. *Inorg. Chim. Acta* 1982, 61, 207.

(4) Koshy, K.; Dasgupta, T. P. *J. Chem. Soc., Dalton Trans.* 1984, 2781.